

~~CONFIDENTIAL~~
~~SECURITY INFORMATION~~

UNCLASSIFIED

CENTRAL RESEARCH LIBRARY
DOCUMENT COLLECTION

DECLASSIFIED

CLASSIFICATION CHANGED TO:
BY AUTHORITY OF: T.D.-111
BY: K. Page 10/26/56

ORNL-1124
Physics and Math.

MARTIN MARIETTA ENERGY SYSTEMS LIBRARIES



3 4456 0360776 4

LABORATORY RECORDS
1954

ANALYSIS OF FLOW THROUGH A SPHERE
FIRST REPORT

OAK RIDGE NATIONAL LABORATORY
CENTRAL RESEARCH LIBRARY
DOCUMENT COLLECTION

LIBRARY LOAN COPY

DO NOT TRANSFER TO ANOTHER PERSON
If you wish someone else to see this
document, send in name with document
and the library will arrange a loan.

UCN-7969
(3 3-67)



OAK RIDGE NATIONAL LABORATORY
OPERATED BY
CARBIDE AND CARBON CHEMICALS COMPANY
A DIVISION OF UNION CARBIDE AND CARBON CORPORATION



POST OFFICE BOX P
OAK RIDGE, TENNESSEE

UNCLASSIFIED

~~CONFIDENTIAL~~
~~SECURITY INFORMATION~~

UNCLASSIFIED

[REDACTED]
ORNL-1124

This document consists of 46 pages.
Copy 8 of 176. Series A

Contract No. W-7405, eng 26

Reactor Experimental Engineering Division

ANALYSIS OF FLOW THROUGH A SPHERE

FIRST REPORT

D. H. Fax
S. C. Traugott
G. F. Wislicenus

Date Issued

FEB 6 1952

OAK RIDGE NATIONAL LABORATORY
Operated by
CARBIDE AND CARBON CHEMICALS DIVISION
Union Carbide and Carbon Corporation
Post Office Box P
Oak Ridge, Tennessee

[REDACTED]
[REDACTED]

[REDACTED]
[REDACTED]



UNCLASSIFIED

3 4456 0360776 4

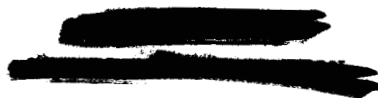


Table of Contents

Introduction ----- v

Outline of the Report ----- vi

Nomenclature ----- ix

1. The Equations of Motion ----- 1

2. The Momentum and Continuity Equations ----- 2

3. The Energy Equation ----- 10

4. Normalization of the Dimensional Quantities ----- 10

5. Simultaneous Solution of the Equations of Motion ----- 13

6. Numerical Integration of the Equation $D^2\psi = -\zeta \cdot r$ ----- 17

7. Integration of the Energy and Momentum Equations ----- 22

8. Frictionless Incompressible Flow (with solutions) ----- 23

Acknowledgments ----- 34

Bibliography ----- 35

List of Figures

1. Definition of the Coordinate Systems ----- 2

2. Effect of Vertical Temperature Gradient on Secondary Flow ----- 8

3. Effect of Radial Temperature Gradient on Secondary Flow ----- 9

4. Effect of Peripheral Boundary Layer on Secondary Flow ----- 10

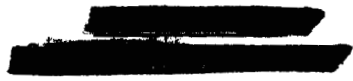
5. Lattice for Numerical Integration of $D^2\psi = -\zeta \cdot r$ ----- 19

6. Solution of Potential Flow - Entry at 30° N. Latitude ----- 24

7. Solution of Potential Flow - Entry at 30° S. Latitude ----- 25

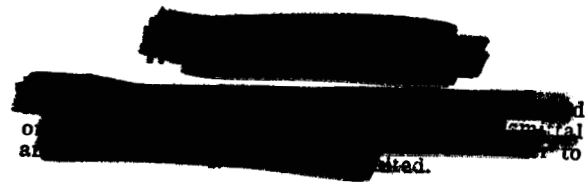
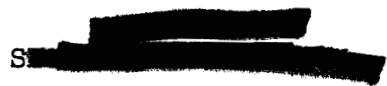
8. Solution of Potential Flow - Entry at 45° S. Latitude ----- 26

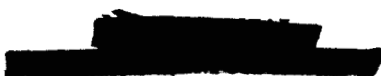
9. Spherical Vortex ----- 29



List of Figures (Continued)

- 10. Frictionless, Incompressible Flow: Entry at 30° N. Latitude,
With Inlet Pipe at 30° to the Radial Direction ----- 31
- 11. Frictionless, Incompressible Flow: Entry at 30° S. Latitude,
Inlet Pipe at 30° to the Radial ----- 32
- 12. Same as (11), but with Inlet Pipe at 11.5° to the Radial ----- 33




Introduction

Predicting the fluid flow pattern in a sphere, under the combined influences of friction and distributed heat sources, is a complicated problem. It is almost trite to say that neither model experiments nor mathematical analysis, one without the other, is very convincing; quite obviously, each must lean heavily on the other.

This report outlines the beginnings of some theoretical work intended to supplement and extend the model experiments performed for the HRE. While the experiments have helped us remarkably in directing the lines along which the analysis must go, and have also indicated the order of magnitude of certain influences which are not readily predictable by analysis but which must be incorporated therein, a satisfactory wedding of the experimental and analytical results has not yet taken place. However, we feel confident enough in our method of attack to predict that such a meeting will eventually take place and to recommend that this work be continued toward that goal.

To make the analysis tractable at all, a number of idealizations must be made. The first is that the flow is completely symmetrical with respect to the axis of rotation. This implies that the inlet, instead of consisting of a single pipe, as in the HRE, is an annulus running around the sphere at a constant latitude. There is evidence from the experiment that this is not too bad an idealization; even with a single inlet, there have been observed no variations with respect to longitude (i.e., peripheral angle). If such variations do exist, but are simply not detectable by present measuring techniques, it can still be said that the idealization will be closer to reality in the case

of larger reactors, for which multiple inlets are planned.

A second idealization is that turbulence is not explicitly taken into account. It is accounted for implicitly in that where the analysis requires information as to the extent and magnitude of the retarded layer near the wall of the sphere, this information is to be taken largely from measurements made on the model sphere, which take into account the action of turbulence. On the other hand, in calculating temperature distribution, the effect of turbulent interchange has so far been neglected. This is imperfect at best, but the results of our analysis should then be viewed as conservative; that is, temperature gradients will in actuality be less than the analysis will predict.

In addition to these two principal idealizations, a number of minor simplifications are made and these are explained in the body of the report.

Outline of the Report

Section 1

The equations of motion (momentum, continuity, and energy equations) are stated in quite general form, in vector notation. The energy equation is immediately simplified for the purposes of the present problem.

Section 2

The momentum and continuity equations are manipulated by vector operations. The generalized curvilinear coordinate system is then introduced. This is done because it will be found convenient to use three different coordinate systems in different parts of the analysis: cylindrical coordinates,

~~CONFIDENTIAL~~
~~SECURITY INFORMATION~~

spherical coordinates, and a system in which the streamlines and their normals form the coordinate directions. The result of all this is equation (16), which describes the effect of retarded layer and temperature gradients on the meridional flow. A physical interpretation of each of the terms of this equation follows immediately after equation (16).

Section 3

The energy equation is further reduced to a form which permits its integration.

Section 4

The variables and parameters appearing in the final equations are normalized, or made dimensionless. This adds power to the analysis because it makes the results of any one calculation applicable to an entire class of dynamically similar systems. For example, the ratio of peripheral to meridional flow is found to be expressible by a single number; this radically reduces the number of independent variables required to define the system. Only two other dimensionless numbers are required to define the dynamics of a given geometrical configuration; one describes the over-all temperature rise of the fluid through the reactor, the other (which probably has little effect on the results) is the ratio of gravitational to centrifugal forces.

Section 5

At this point we have to solve three simultaneous linear partial differential equations in order to find the effects of friction and temperature

~~CONFIDENTIAL~~
~~SECRET~~

gradients on the meridional flow. The solution is not straightforward, but must be done by iteration, or successive approximations. The first method tried has not worked, and it is explained why. However, a calculation of the order of magnitude of the resulting temperature gradients is made and this furnishes a good deal of insight as to the direction in which one must proceed. A new method is proposed for future trial, and its expected advantages are discussed.

Sections 6 and 7

The details of numerical integration of the three equations are discussed. The differential equations are replaced by finite-difference equations and electronic calculating machines are employed in the solution.

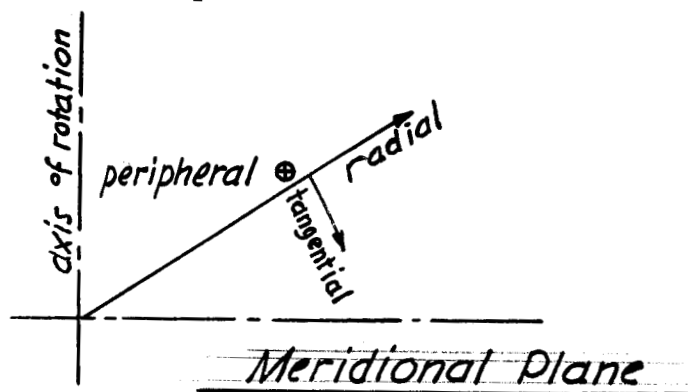
Section 8

The area in which we had considerable success is in the solution of the frictionless incompressible flow for various inlet configurations. This requires the solution of only one of the three differential equations described above. Results of such calculations for several configurations of interest are presented. These results, while not presuming to describe the real flow pattern, are a necessary starting point for the understanding of the general problem.

\vec{v}	velocity vector
z	distance, measured upward from the equator, along the axis of rotation
α, β, γ	generalized curvilinear coordinates
β	volumetric coefficient of expansion
δ_0	angle between the axis of the inlet pipe and the radial direction, measured in the meridional plane
Δ	finite difference
$\nabla, \nabla \cdot, \nabla \times$	vector operators: gradient, divergence and curl
∇^2	Laplacian operator
θ	in spherical coordinates, angle measured from the N-pole
μ	absolute viscosity, mass/length, time
ν	kinematic viscosity, μ/ρ , length ² /time
ξ, η, ζ	orthogonal components of the vorticity vector, (time) ⁻¹
ρ	density
Φ	viscous dissipation of energy/unit volume, time
ψ	stream function, volume/time
$\vec{\omega}$	vorticity vector, $\nabla \times \vec{v}$
Ω	angular momentum per unit mass = rW , where W is the peripheral component of velocity

Primed quantities are normalized as described in Section 4.

Subscript zero denotes conditions at the inlet.



1. The Equations of Motion

The equations of motion for a viscous compressible fluid are: the momentum equation

$$\frac{D\vec{v}}{Dt} = \frac{\partial \vec{v}}{\partial t} + \frac{1}{2} \nabla(\vec{v})^2 - (\vec{v} \times \vec{\omega}) = \vec{F} - \frac{1}{\rho} \nabla p - \nu (\nabla \times \vec{\omega}) + \frac{4}{3} \nu \nabla(\nabla \cdot \vec{v}), \quad (1)$$

the equation of continuity

$$\frac{\partial \rho}{\partial t} + \nabla \cdot (\rho \vec{v}) = 0, \quad (2)$$

and the energy equation

$$\rho \frac{DH}{Dt} = \frac{Dp}{Dt} + k \nabla^2 T + \Phi + q, \quad (3)$$

where

H = enthalpy/unit mass

k = thermal conductivity

Φ = energy dissipation/unit volume, unit time

$$= \mu \left\{ (\vec{\omega})^2 + 2 \nabla \cdot [(\vec{v} \cdot \nabla) \vec{v}] - 2 \vec{v} \cdot \nabla(\nabla \cdot \vec{v}) - \frac{2}{3} (\nabla \cdot \vec{v})^2 \right\}$$

q = internal heat generated/unit volume, unit time.

In equation (3), the four terms on the right side describe the enthalpy rise of the fluid due, respectively, to compressive effects, thermal conduction within the fluid, viscous dissipation, and heat generation. In

the present case, the first three are negligibly small compared with the fourth. Furthermore, replacing dH by $c_p dT$ (presuming the fluid to remain in the liquid state) equation (3) simplifies to

$$\frac{DT}{Dt} = g / \rho c_p \quad (4)$$

2. The Momentum and Continuity Equations

Following Goldstein (Ref. 1), except that density variations are here not neglected, equations (1) and (2) are reduced as follows: Taking the curl of (1) and dropping time-dependent terms:

$$\nabla \times (\vec{v} \times \vec{\omega}) = \nabla \frac{1}{\rho} \times \nabla p + \nabla \times (\nabla \times \vec{\omega}) \quad (5)$$

For steady-state axi-symmetric flow, equation (2) can be satisfied by the definition of a stream function ψ . It is convenient to use a generalized coordinate system (α, β, γ) , where the elemental displacements are given by $h_1 d\alpha, h_2 d\beta, h_3 d\gamma$. With reference to Figure 1, z is the axis

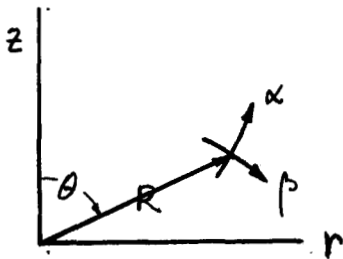


FIG. 1

of rotation, θ is the angle measured from the N-pole, R is the radius from the center of the sphere, r is the distance from the axis of rotation; and for a right-handed system, the positive direction of γ is into the plane in the first and fourth quadrants of the meridional plane.

Because of axi-symmetry, $\frac{\partial}{\partial \gamma} = 0$; $h_3 = r = R \sin \theta$. In cylindrical coordinates, $\alpha = z$ and $\beta = r$, $h_1 = 1$ and $h_2 = 1$. In spherical

coordinates, $\alpha = R$ and $\beta = \theta$, $h_1 = 1$ and $h_2 = R$. The components of the velocity vector will be denoted by u, v, w in the directions α, β, γ , respectively; the components of the vorticity vector are ξ, η, ζ .

In defining a stream function ψ to satisfy equation (2), no significant accuracy is lost by neglecting the variation in density over the field. Were the density variation included here, terms would be introduced in later equations which would be quite negligible compared with the other terms in those equations, and no gain would result from the added complication. However, it must be emphasized that the first term on the right of equation (5) cannot be neglected; there it is found that in this problem the coefficient of the density gradient is quite large and the whole term becomes of the first magnitude.

Returning to equation (2),

$$\rho \nabla \cdot \vec{v} = \frac{\rho}{h_1 h_2 h_3} \left[\frac{\partial}{\partial \alpha} (h_2 h_3 u) + \frac{\partial}{\partial \beta} (h_1 h_3 v) \right] = 0 \quad (6)$$

which is satisfied by

$$u = \frac{1}{h_2 h_3} \frac{\partial \psi}{\partial \beta} \quad \text{and} \quad v = -\frac{1}{h_1 h_3} \frac{\partial \psi}{\partial \alpha} \quad (7)$$

It is convenient to replace the peripheral component w by the angular momentum per unit mass, Ω , i.e.,

$$\Omega = h_3 \omega . \quad (8)$$

The vorticity vector

$$\vec{\omega} = \nabla \times \vec{V} = \frac{1}{h_1 h_2 h_3} \begin{vmatrix} h_1 \vec{e}_1 & h_2 \vec{e}_2 & h_3 \vec{e}_3 \\ \frac{\partial}{\partial \alpha} & \frac{\partial}{\partial \beta} & \frac{\partial}{\partial \gamma} \\ h_1 u & h_2 v & h_3 w \end{vmatrix} ,$$

from which the three vorticity components are, using equations (7) and (8),

$$\xi = \frac{1}{h_2 h_3} \frac{\partial \Omega}{\partial \beta} , \quad (9)$$

$$\eta = -\frac{1}{h_1 h_3} \frac{\partial \Omega}{\partial \alpha} , \quad (10)$$

and

$$\xi = -\frac{1}{h_1 h_2} \left[\frac{\partial}{\partial \alpha} \left(\frac{h_2}{h_3 h_1} \frac{\partial \psi}{\partial \alpha} \right) + \frac{\partial}{\partial \beta} \left(\frac{h_1}{h_2 h_3} \frac{\partial \psi}{\partial \beta} \right) \right] = -\frac{1}{h_3} D^2 \psi , \quad (11)$$

where

$$D^2 \equiv \frac{h_3}{h_1 h_2} \left[\frac{\partial}{\partial \alpha} \left(\frac{h_2}{h_3 h_1} \frac{\partial}{\partial \alpha} \right) + \frac{\partial}{\partial \beta} \left(\frac{h_1}{h_2 h_3} \frac{\partial}{\partial \beta} \right) \right] .$$

{ Note that D^2 is an operator which is adjoint to the Laplacian, which is

$$\nabla^2 \equiv \frac{1}{h_1 h_2 h_3} \left[\frac{\partial}{\partial \alpha} \left(\frac{h_2 h_3}{h_1} \frac{\partial}{\partial \alpha} \right) + \frac{\partial}{\partial \beta} \left(\frac{h_1 h_3}{h_2} \frac{\partial}{\partial \beta} \right) \right]$$

In Cartesian coordinates, where $h_1 = h_2 = h_3 = 1$, D^2 and ∇^2 are identical. }

Equation (5) is the equation for the vorticity. The third component of vorticity, ξ , is the one which produces secondary flow in the meridional plane. Taking the third component of equation (5),

$$\frac{1}{h_1 h_2} \left[\frac{\partial(\psi, \xi/h_3)}{\partial(\alpha, \beta)} + \frac{2\Omega}{h_3} \frac{\partial(\Omega, h_3)}{\partial(\alpha, \beta)} \right] = \frac{1}{h_1 h_2} \frac{\partial(\frac{1}{\rho}, p)}{\partial(\alpha, \beta)} + \frac{\nu}{h_3} D^2(D^2\psi), \quad (12)$$

where $\frac{\partial(\cdot, \cdot)}{\partial(\cdot, \cdot)}$ is the Jacobian operator.

Another independent equation between ψ and Ω is required and this is obtained by taking the third component of equation (1). Noting that $(\vec{F})_3 = 0$, $\frac{\partial}{\partial y} = 0$, and using equations (7), (9), and (10),

$$\frac{1}{h_1 h_2 h_3} \frac{\partial(\psi, \Omega)}{\partial(\alpha, \beta)} = -\nu D^2\psi. \quad (13)$$

The last two equations may be interpreted as follows: The first term of (12) describes the growth of vorticity in the meridional plane; the second term, production of this vorticity due to the boundary layer of the peripheral flow; the third term, production due to density gradients; the last term, production due to viscosity acting on the meridional flow. The last term must be quite small compared with the others; it will be neglected in the remainder of this discussion.

Equation (13) describes the effect of viscosity acting on the peripheral flow and must be solved simultaneously with equation (12). This does not appear at present to be within reach. Instead, a simpler and more realistic attack is proposed, that of making an assumption as to the magnitude of a peripheral flow boundary layer, based largely upon direct measurements made on the plastic model, and inserting this assumption into equation (12).

This procedure has several recognized difficulties: (a) the measurements themselves are quite difficult to make in that the support for the probe inevitably disturbs the flow in the sphere; (b) the boundary layer will itself change under the influence of density gradients in the fluid, and this cannot be duplicated in the plastic model; and (c) investigation of the effects on boundary layer of different inlet arrangements requires either a number of different plastic models or extrapolation from the one set of data which itself is of rather low accuracy. Nevertheless, this procedure appears at present to be more attractive than the alternative mentioned at the beginning of this paragraph.

Returning to equation (12), it can be shown that each of the terms is invariant with respect to different sets of (α, β) provided, of course, that in each term α and β are orthogonal and the h 's be defined according to the respective definitions of α and β . Thus in the first term, it appears at present to be convenient to choose α and β in the directions normal to and along the streamlines, respectively, so that $\frac{\partial}{h_1 \partial \alpha} = \frac{\partial}{\partial n}$ and $\frac{\partial}{h_2 \partial \beta} = \frac{\partial}{\partial s}$. In the second and third terms, it is more convenient to choose $\alpha = z$ and $\beta = r$, thus $h_1 = h_2 = 1$. In each case $h_3 = r = R \sin \theta$, the distance from the axis of rotation. Neglecting the viscosity term, and noting that $\partial \psi / \partial s = 0$, (12) becomes

$$\left(\frac{\partial \psi}{\partial n} \right) \frac{\partial (k/r)}{\partial s} = - \frac{1}{r^3} \frac{\partial (\Omega^2)}{\partial z} + \frac{\partial (1/r)}{\partial z} \frac{\partial p}{\partial r} - \frac{\partial (1/r)}{\partial r} \frac{\partial p}{\partial z} \quad (14)$$

Note that to be consistent with the definition of ψ in equation (7), $\frac{\partial \psi}{\partial n}$ is always negative; $-\frac{1}{r} \frac{\partial \psi}{\partial n}$ is the velocity along the streamline in the positive direction. The first term on the right may also be written

$$\left[- \frac{\partial (w^2/r)}{\partial z} \right]$$

To evaluate the last two terms in equation (14), a further linearization is necessary. The r and z components of equation (1) are, omitting derivatives with respect to the peripheral angle and neglecting the viscous terms,

$$v \frac{\partial v}{\partial r} + u \frac{\partial v}{\partial z} - \frac{w^2}{r} = -\frac{1}{\rho} \frac{\partial p}{\partial r} \quad (15a)$$

and

$$u \frac{\partial u}{\partial z} + v \frac{\partial u}{\partial r} = -\frac{1}{\rho} \frac{\partial p}{\partial z} - g \quad (15b)$$

It appears reasonable to say that the pressure field is determined principally by the centrifugal and gravitational fields respectively, and that the perturbations on the pressure field due to the meridional flow when multiplied by the density gradients give higher order terms which are negligible in equation (14). For the purposes of equation (14), therefore, $\frac{\partial p}{\partial r} \doteq \rho_0 \frac{w^2}{r}$ and $\frac{\partial p}{\partial z} \doteq -\rho_0 g$, where ρ_0 is a constant density evaluated, say, at the inlet.

The density gradients may be translated into temperature gradients through the volumetric coefficient of expansion, β ;

$$\beta = -\frac{1}{\rho} \left(\frac{\partial \rho}{\partial T} \right)_p \doteq \frac{\rho_0 - \rho}{\rho(T - T_0)} \quad \text{for small density changes,}$$

where subscript zero denotes inlet conditions. From this,

$$\frac{\partial(1/\rho)}{\partial z} = \frac{\beta}{\rho_0} \left(\frac{\partial T}{\partial z} \right) \quad \text{and} \quad \frac{\partial(1/\rho)}{\partial r} = \frac{\beta}{\rho_0} \left(\frac{\partial T}{\partial r} \right).$$

Equation (14) now becomes

$$\frac{\partial \psi}{\partial n} \frac{\partial(\zeta/r)}{\partial s} = -\frac{1}{r^3} \frac{\partial(\Omega^2)}{\partial z} + \beta \left[\frac{w^2}{r} \frac{\partial T}{\partial z} + g \frac{\partial T}{\partial r} \right] \quad (16)$$

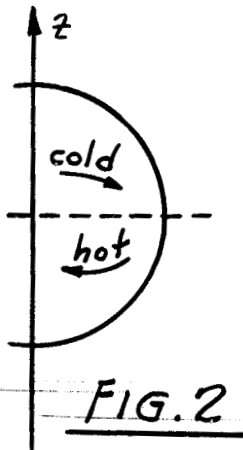
~~SECURITY INFORMATION~~

Equation (16) shows explicitly how the potential (frictionless, incompressible) flow is distorted by the effects of friction and temperature gradients.

In the term on the left, $-\frac{\partial \psi}{\partial n}$, except for a factor of r , is proportional to the meridional velocity, whereas $\frac{\partial(\xi/r)}{\partial s}$ is the rate of growth (along a streamline) of the vorticity vector normal to the meridional plane. This vorticity vector represents the departure of the meridional streamlines from the potential solution, and thus is a measure of the secondary flow.

The physical mechanism of this effect is as follows:

Considering first the temperature gradients, $\frac{w^2}{r} \frac{\partial T}{\partial z}$ is the product of the vertical temperature gradient and the centripetal acceleration. That such a factor should produce a rotational flow in the meridional plane is seen by examining Figure 2. Imagine a crude temperature distribution as shown.



Then, with rotation of the fluid about the z axis, the upper, cold fluid portion, having a higher density, will tend to move outwards to maintain radial equilibrium between centrifugal force and static pressure. Just the opposite is true for the lower, warm portion, and thus a clockwise circulating motion (positive vorticity ξ)

is created. Obviously, a counterclockwise circulating motion would result for the reverse temperature distribution.

~~CONFIDENTIAL~~

The term $g \frac{\partial T}{\partial r}$ is the product of the radial temperature gradient and the gravitational field. For a temperature distribution as shown in Figure 3



FIG. 3

it is seen that, due to the larger density in the outer region, a clockwise circulatory motion results. Again, reversal of the warm and cold portions would reverse the direction of rotation.

It is believed that, since the centrifugal forces greatly exceed gravitational forces in the present application, the term $\frac{w^2}{r} \frac{\partial T}{\partial z}$ will exceed $g \frac{\partial T}{\partial r}$. This will not be true, of course, if the radial temperature gradient becomes somewhere in the field much larger than the vertical temperature gradient, but this appears unlikely.

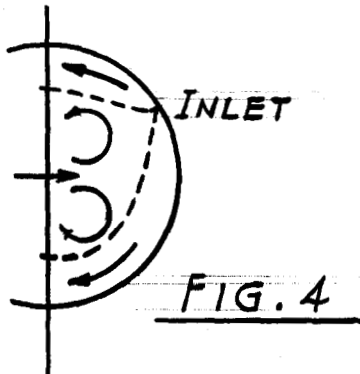
As will be seen later, the potential solution for a radial inlet in the upper hemisphere shows much higher velocities in the upper portion of the reactor than in the lower. This would indicate negative vertical temperature gradients, and a resulting clockwise circulating motion as roughly indicated in Figure 2. This would then reduce the velocity in the upper portion, giving a higher temperature there. In the lower portion, the velocity is increased and the temperature reduced by this secondary motion.

Thus, large temperature gradients would tend to be reduced by the creation of a secondary motion generated by these gradients. The magnitude of this effect depends on the magnitude of the centrifugal forces, as previously indicated.

[REDACTED]

The term describing the effect of vertical gradients in the peripheral velocity component due to the influence of fluid friction is $\frac{1}{r^3} \frac{\partial(\Omega^2)}{\partial z}$

Figure 4 shows a possible friction layer near the walls, indicating a region of reduced peripheral velocity, w . In the upper and lower regions a reduction



in peripheral velocity $W = \frac{\Omega}{r}$ gives rise to an inward motion of the fluid, again in order to maintain radial equilibrium. In this case, however, two vortices are generated rather than just one, the upper one negative and the lower positive.

It becomes apparent that in the lower portions of the reactor the actions of fluid friction and varying density reinforce each other, while at the top these two influences act in opposite directions.

3. The Energy Equation

Equation (4) may be written

$$\frac{DT}{Dt} = \frac{\partial T}{\partial t} + \frac{1}{h_1 h_2 h_3} \left(\frac{\partial T}{\partial \alpha} \frac{\partial \psi}{\partial \beta} - \frac{\partial T}{\partial \beta} \frac{\partial \psi}{\partial \alpha} \right) = g / \rho c_p. \quad (17)$$

Taking α and β in the directions normal to and along the streamlines, respectively, this reduces to

$$- \frac{\partial \psi}{\partial n} \frac{\partial T}{\partial s} = g r / \rho c_p. \quad (18)$$

4. Normalization of the Dimensional Quantities

We have left a set of three simultaneous equations, (11), (16), and (18) for the three unknowns ψ , ξ , and T . (Note that while ξ could be

eliminated by substituting its defining equation (11) into (16), this would yield a third order second degree equation in ψ , which would be rather difficult to solve directly.) Before proceeding with any computations, it is convenient to normalize the variables and reduce all the terms to dimensionless groupings.

All of the linear dimensions may be normalized with respect to the outside radius, i.e., $R' = R/R_0$, $r' = r/R_0$, $s' = s/R_0$, $n' = n/R_0$. The temperature rise from the inlet to any point in the sphere is normalized with respect to the average temperature rise from inlet to outlet, i.e.,

$T' = (T - T_0) / \Delta T_{ave}$. The stream function is normalized with respect to the total through flow, i.e., $\psi' = 2\pi\psi/Q$, where Q is the total through flow in cfs. The angular momentum is normalized with respect to that at the inlet; $\Omega' = \Omega/\Omega_0$.

The source function g is normalized with respect to the average source taken over the sphere, i.e., $g' = g/g_{ave}$. This is convenient because the relation

$$\frac{4}{3} \pi R_0^3 g_{ave} = \rho c_p Q \Delta T_{ave} \quad (19)$$

permits the elimination of the terms g_{ave} , ρ , and c_p ; in other words, the power level will be specified indirectly through the terms Q and ΔT_{ave} .

According to Reference (2), the source distribution as a function of R' may in the present case be approximated by a parabola with a zero slope at $R' = 0$ and a value of 26.5% of the maximum at $R' = 1$. Averaging this parabola over the sphere and normalizing, yields

$$g' = 1.790 - 1.317 (R')^2 \quad (20)$$

Summing up in dimensionless form, the three equations become

(a) the energy equation

$$T' = 1.5 \int_{(s)} \frac{g' r'}{\rho - \frac{\partial \psi'}{\partial n'}} ds' \quad , \quad (21)$$

(b) the vorticity equation

$$\left(\frac{f}{r}\right)' = \int_{(s)} \frac{\frac{1}{r'^3} \frac{\partial (\Omega')^2}{\partial z'} - (\beta \Delta T_{ave}) \left[\frac{\Omega'^2}{r'^3} \frac{\partial T'}{\partial z'} + g \frac{R_0^3}{\Omega_0^2} \frac{\partial T'}{\partial r'} \right]}{-\partial \psi' / \partial n'} ds' \quad , \quad (22)$$

and (c) the relation between vorticity and stream function

$$D^2 \psi' \equiv \frac{\partial^2 \psi'}{\partial R'^2} + \frac{\sin \theta}{R'^2} \frac{\partial}{\partial \theta} \left(\frac{1}{\sin \theta} \frac{\partial \psi'}{\partial \theta} \right) = - \left(\frac{2\pi \Omega_0 R_0}{Q} \right)^2 \left(\frac{f}{r} \right)' R'^2 \sin^2 \theta \quad . \quad (23)$$

The dimensionless groupings, therefore, which characterize the flow are: $\beta \Delta T_{ave}$; $g R_0^3 / \Omega_0^2$, which is proportional to the ratio of gravitational forces to centrifugal forces; and $(2\pi \Omega_0 R_0 / Q)^2$, which characterizes the ratio of the centrifugal forces to the inertia forces in the meridional plane. This latter group is really the reciprocal of a kind of Froude's number, which is perhaps made more obvious by rewriting it as $4 \left(\frac{W_0^2}{R_0} \right) R_0 / \left(\frac{Q}{\pi R_0^2} \right)^2$. Froude's number is generally defined as $v^2 / L g$, the ratio of inertia to gravity forces; in the present instance, W_0^2 / R_0 replaces the gravity field while $Q / \pi R_0^2$ describes the meridional velocity (based on the area of a great circle).

The product $(\beta \Delta T_{ave}) \left(\frac{2\pi \Omega_0 R_0}{Q} \right)^2$ yields a group which is frequently called Weber's expansion number; it describes the ratio of the buoyant to the inertia forces.

5. Simultaneous Solution of the Equations of Motion

The procedure presently proposed for the simultaneous solution of equations (21), (22), and (23) is as follows:

(a) Assume a set of streamlines over the field, consistent with the prescribed boundary conditions.

(b) From equation (21), perform the indicated integration along successive streamlines to find the temperature distribution corresponding to the assumed field of flow. The initial condition for this integration is, of course, $T' = 0$ at the inlet for each of the streamlines; T' at the outlet end of each streamline is a dependent variable, but if the work

is done carefully, $\int_{\psi'=0}^{\psi'=1} T' d\psi'$ taken across the outlet should come out to be unity.

(c) From the resultant temperature distribution and the measured (or assumed) distribution of peripheral velocity, integrate along streamlines to find the vorticity, according to equation (22). The initial condition is again $(\xi/r)' = 0$ at the inlet, which assumes that the inlet flow is irrotational, or has negligible vorticity compared with that produced in the sphere.

(d) Having the distribution of vorticity, integrate equation (23), a linear second-order partial differential equation, to find the streamlines, ψ .

(e) Having now a new set of streamlines, presumably better than the initial assumption, return to (a) and repeat the process until convergence is obtained.

[REDACTED]

The actual techniques of performing the individual integrations will be discussed in the next section; first, the procedure described above will be examined in more detail.

At the outset let us say that at the present writing we have not yet found a numerical solution to the complete set of three equations; that is, we have not made the system converge. From the work we have done, it appears that the initial assumption of the distribution of ψ must lie within a certain neighborhood of the ultimate solution in order for the system of equations to converge; this region of convergence becomes smaller and smaller as the values of the governing parameters $\beta \Delta T_{ave}$ and $(2\pi \Omega_0 R_0 / Q)^2$, get larger. With the values of the parameters as prescribed in the HRE, the region of convergence is apparently so small that we have not yet found it. Until one can make an assumption which proves to be inside this region, the procedure described above is a cut-and-try process, rather than an iterative one.

To point this out more clearly, let us assume that one might take the potential (i.e., frictionless and incompressible) solution for ψ as the first assumption in (a), with the hope that gradients in angular momentum and temperature will produce only minor perturbations in the potential solution. The potential solution for entry at $\theta = 60^\circ$ (i.e., 30° north latitude) with no tangential component at the inlet (but only radial and peripheral components) is shown in Figure 6. Using this solution as a starting point, equation (21) gives tremendous temperature differences over the field, due to the great disparities in residence time as revealed by the streamlines. For example, at $r' = 0.5$, the value of T' along the upper arc of the meridian has

[REDACTED]
[REDACTED]

reached only 0.10 (i.e., 10% of the rated average temperature rise through the reactor), while at the same radius T' along the lower arc is about 8.4. This corresponds to an "average" temperature gradient in the vertical direction of $\frac{\delta T'}{\delta z'} = -5$, roughly. (To translate this into degrees/unit length, multiply the number by $\Delta T_{ave}/R_o$.) When inserted into equation (22) and then into (23), it is revealed that the resulting vorticity is so large that the through-flow is almost completely dominated by a large vortex, giving a closed region in the center of the sphere. This is obviously no good for the next iteration since the steady-state temperature in this closed region would be unbounded; in other words, we are far outside the range in which our linearizations remain valid.

A rough calculation shows that in order to avoid such closed regions with the configuration described above, it is necessary that the "average" vertical temperature gradient be in the neighborhood of - 0.006 or less (in absolute magnitude) as compared with the - 5. mentioned in the preceding paragraph. (The figure of - 0.006 is based on the magnitudes of the flow parameters prescribed for the HRE.)

This rough calculation teaches two things: (a) With a strong peripheral velocity/meridional velocity ratio, as here prescribed, there is a strong influence which keeps vertical temperature gradients very small. This is very favorable provided it can be shown that this influence is a stable one rather than one which leads to oscillating temperatures. (b) The convergence of the mathematical procedure described above is extremely sensitive to the first assumption of streamlines.

This naturally begs the question: Is the order of solution given above the best order for solving equations (21), (22), and (23), or would another order give a process with less sensitivity to the original assumption? We feel at present that the proposed method is the best for the following reasons. The procedure described above (page 13) can be condensed to:

- (a) Assumption of ψ'
- (b) Differentiation followed by integration in equation (21) to obtain T'
- (c) Differentiation followed by integration in equation (22) to obtain $(\epsilon/r)'$
- (d) Double integration in equation (23), yielding new values of ψ' .

The inverse procedure to that proposed would be:

- (a) Assumption of ψ'
- (b) Differentiation followed by integration in equation (21) to obtain T'
- (c) Double differentiation of ψ' in (23) to obtain $(\epsilon/r)'$
- (d) Differentiation followed by integration in (22) to obtain new ψ' 's.

The significant difference between the two procedures is triple integration vs. triple differentiation of the original assumption. It appears clear that the former must be a "smoother" process than the latter.

We are left with the problem of making the procedure described on page 13 less sensitive to initial assumption. We feel that the method described below, although as yet untried, has strong chances of success.

~~CONFIDENTIAL~~

The newly proposed method is to use the same procedure as before, in principle if not in detail, starting perhaps with the potential solution as a first guess for ψ' , down to the calculation of the new ψ' 's from equation (23). In this step, however, instead of using the value of the parameter $\left[2\pi\Omega_0 R_0/Q\right]^2$ prescribed in the HRE, solve for a value of this parameter which gives a secondary flow which only perturbs the first assumption instead of dominating it completely. This will yield a new meridional flow which can be used in the next cycle of the iteration. It is anticipated that on each successive cycle, the value of $\left[2\pi\Omega_0 R_0/Q\right]^2$ can be progressively increased, each small jump perturbing the preceding solution, until the full prescribed value is reached. This method consists, in a sense, of starting with a large region of convergence and then letting that region shrink in such a way that one always remains just inside the boundary of the region as one approaches the final solution.

The proposed method has another very important advantage. For each value of the gradually increasing parameter, it should be no trick to solve for the appropriate streamline configuration which satisfied the equations for that value of the flow parameter. This will give a family of solutions for a wide range of $\left[2\pi\Omega_0 R_0/Q\right]^2$. This information is particularly important for the design of future reactors, larger than the HRE, where the ratio of peripheral to meridional velocities must be considerably less than in the HRE because of pressure drop considerations.

6. Numerical Integration of the Equation $D^2\psi = -\xi r$

Equation (23),

$$D^2\psi' \equiv \frac{\partial^2\psi'}{\partial R'^2} + \frac{\sin\theta}{R'^2} \frac{\partial}{\partial\theta} \left(\frac{1}{\sin\theta} \frac{\partial\psi'}{\partial R'} \right) = - \left(\frac{2\pi\Omega_0 R_0}{Q} \right)^2 \left(\frac{\xi}{r} \right)' R'^2 \sin^2\theta ,$$

is written in spherical coordinates because it is easiest in this system to fit the prescribed boundary conditions on ψ' . The method of integration consists of replacing the partial differential equation by a large number of algebraic finite difference equations involving the values of ψ' at certain interior joints. Simultaneous solution of these equations yields the distribution of ψ' . The more interior points that are used, the more the resulting accuracy, and the more labor.

Referring to Figure 5, consider the half-circle ($0 \leq \theta \leq \pi$, $0 \leq R' \leq 1$) divided into a lattice of uniform $\Delta\theta$'s and $\Delta R'$'s. The coordinates of a given point on the lattice are (R_i, θ^j) . (Primes will be dropped temporarily to avoid confusion with the i, j notation.) Neighboring points of interest are (R_{i-1}, θ^j) , (R_{i+1}, θ^j) , (R_i, θ^{j-1}) , and (R_i, θ^{j+1}) . Writing the Taylor series expansions for ψ_{i+1}^j and ψ_{i-1}^j , each in terms of ψ_i^j , and adding the two expansions, one finds

$$\left(\frac{\partial^2 \psi}{\partial R^2}\right)_{i,j} = \frac{\psi_{i+1}^j + \psi_{i-1}^j - 2\psi_i^j}{(\Delta R)^2} - \frac{(\Delta R)^2}{12} \left(\frac{\partial^4 \psi}{\partial R^4}\right)_{i,j} + \dots \quad (24)$$

In a similar manner, it can be shown that

$$\left[\frac{\partial}{\partial \theta} \left(\frac{1}{\sin \theta} \frac{\partial \psi}{\partial \theta}\right)\right]_{i,j} = \frac{1}{(\Delta \theta)^2} \left[\frac{\psi_i^{j+1} - \psi_i^j}{\sin(\theta^j + \frac{\Delta \theta}{2})} + \frac{\psi_i^{j-1} - \psi_i^j}{\sin(\theta^j - \frac{\Delta \theta}{2})} \right] - \frac{(\Delta \theta)^2}{24} \left\{ \left[\frac{\partial^3}{\partial \theta^3} \left(\frac{1}{\sin \theta} \frac{\partial \psi}{\partial \theta}\right)\right]_{i,j} - \frac{1}{8} \left[\frac{\partial^4 \psi}{\partial \theta^4}\right]_{i,j+\frac{1}{2}} - \frac{1}{8} \left[\frac{\partial^4 \psi}{\partial \theta^4}\right]_{i,j-\frac{1}{2}} \right\} + \dots \quad (25)$$

Substituting equations (24) and (25) into (23),

$$R_i^2 \left(\frac{\Delta \theta}{\Delta R}\right)^2 \left[\psi_{i+1}^j + \psi_{i-1}^j - 2\psi_i^j \right] + \frac{\sin \theta^j}{\sin(\theta^j + \frac{\Delta \theta}{2})} (\psi_i^{j+1} - \psi_i^j) + \frac{\sin \theta^j}{\sin(\theta^j - \frac{\Delta \theta}{2})} (\psi_i^{j-1} - \psi_i^j) + (\Delta \theta)^2 (E_R + E_\theta) = - \left(\frac{2\pi \rho_0 R_0}{Q}\right)^2 \left(\frac{\epsilon}{r}\right)_i^j (\Delta \theta)^2 R_i^4 \sin^2 \theta^j \quad (26)$$

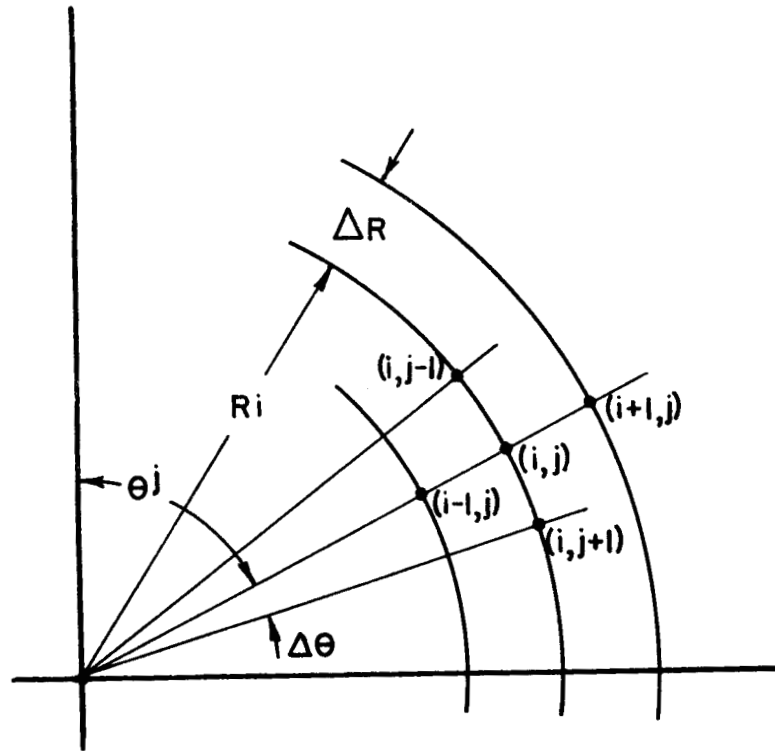


Fig. 5
LATTICE FOR NUMERICAL INTEGRATION
OF $D^2\psi = \xi \cdot r$

where E_R = error involved in the finite difference approximation to $\partial^2 \psi / \partial R^2$, and is of order $(\Delta R)^2$,
 E_θ = error involved in the approximation to $\frac{\partial}{\partial \theta} \left(\frac{1}{\sin \theta} \frac{\partial \psi}{\partial \theta} \right)$, and is of order $(\Delta \theta)^2$

These considerations show that as the lattice spacing is decreased, holding $\Delta \theta / \Delta R$ constant, the error decreases as the square of the lattice dimension. By trying a few combinations, it was found that a lattice spacing of $\Delta R' = 0.1$ and $\Delta \theta = \pi/24$ gives a good approximation to the wanted function.

Rewriting equation (26) with the omission of the error terms,

$$R_i^2 \left(\frac{\Delta \theta}{\Delta R} \right)^2 [\psi_{i+1}^j + \psi_{i-1}^j] + \frac{\sin \theta^j}{\sin(\theta^j + \frac{\Delta \theta}{2})} \psi_i^{j+1} + \frac{\sin \theta^j}{\sin(\theta^j - \frac{\Delta \theta}{2})} \psi_i^{j-1} - \left[2 R_i^2 \left(\frac{\Delta \theta}{\Delta R} \right)^2 + \frac{\sin \theta^j}{\sin(\theta^j + \frac{\Delta \theta}{2})} + \frac{\sin \theta^j}{\sin(\theta^j - \frac{\Delta \theta}{2})} \right] \psi_i^j = - (\Delta \theta)^2 R_i^4 \sin^2 \theta^j \left(\frac{2\pi \Omega_0 R_0}{Q} \right)^2 \left(\frac{\xi}{r} \right)_i^j \quad (27)$$

an equation explicit in ψ_i^j . (The primes are suppressed, but all the quantities are still dimensionless.) For the lattice spacing chosen, there are 207 such linear algebraic equations to be solved simultaneously for each set of boundary conditions in ψ' and distribution of $(\xi/r)^j$.

The solution of this large set of equations is best accomplished on automatic calculating machines. During this past summer, three such problems (potential solutions with inlets at $\theta = 60^\circ$, 120° , and 135° , respectively) were solved in the IBM Card-programmed Electronic Calculator at K-25. The method used, known as the Gauss-Seidel method, starts from an initial

UNCLASSIFIED

[REDACTED]

estimate of the solution to the set of equations, and by a series of iterations, corrects the initial estimate in the direction of the final solution. The number of iterations required depends on the excellence of the initial estimate, on the relative magnitudes of the coefficients of ψ' in the equations, and on the precision to which the solution is required.

With the present problem, the time required per iteration by the CPEC is 90 minutes. In order to obtain reasonable convergence within five or six iterations, it was found that an initial estimate based on intuition was not usually good enough. It was found necessary to base the initial estimate on the results of a hand-calculation of equations (27) based on a course net $(\Delta R = 0.2, \Delta \theta = \frac{\pi}{12})$ with 44 interior points. Using the relaxation techniques described by Southwell (Ref. 3), a reasonably experienced operator can prepare such an estimate in about eight hours.

Following the machine calculation of the ψ' s at the 207 lattice points, it is necessary to plot on the semi-circle the streamlines, or lines of constant ψ . To aid in this, the CPEC performs an interpolation along lines of constant i and j respectively to give values of ψ at $(i, j + \frac{n}{5})$ and at $(i + \frac{n}{5}, j)$, where $n = 1, 2, 3, 4$, for each value of (i, j) . Quadratic, or three-point, interpolation is used. This makes it quite simple to select and plot the coordinates of points of constant ψ .

The CPEC, while quite flexible in its applications, is apparently not the machine best suited for this problem. The NEPA Digital Computer, unavailable this summer, is specifically designed to solve problems of this type. Instead of 90 minutes per iteration, the NEPA Computer can make about 5 iterations

~~CONFIDENTIAL INFORMATION~~

per hour on a set of 207 equations and can reduce the time required to make the initial estimate to about one or two hours. It is urgently recommended that the NEPA Computer be made available to this problem if the work is to be continued.

7. Integration of the Energy and Momentum Equations

Equations (21) and (22) are written to indicate integrations along the streamlines. While simple in principle, this can become "messy" in execution, particularly if good precision is required. An examination of the two equations shows that precision is necessary; after integration along streamlines to find T' , it is necessary to find the vertical and horizontal directional derivatives of T' , and small errors in the integration are greatly magnified in the differentiation.

Another disadvantage of integration along streamlines is that the values of $(\xi/r)'$ so found must then be interpolated to values on the lattice-points for use in equation (23) (or equation (27)). This interpolation can be a nuisance, especially since the vorticity gradients are quite high in some regions of the field.

While some of the details remain to be worked out, we feel that these difficulties can be removed by rewriting equations (21) and (22) so as to require integration along lines of constant R and θ , respectively, rather than along lines of constant ψ . This will have the two-fold advantage of replacing the graphical part of the work by numerical work, and of giving the values of $(\xi/r)'$ directly on the lattice points without interpolation.

8. Frictionless Incompressible Flow (with solutions)

Under the limiting assumption that the fluid has no viscosity, one sees from equation (13) that the angular momentum Ω of the peripheral flow is constant over the field; that is, the peripheral flow is a free vortex. If one couples with this the assumption that the coefficient of expansion β is zero, one finds from equation (22) that the value of ξ/r is constant along each streamline and, in particular, if the vorticity is zero at the inlet, it is zero everywhere. Thus equation (23) reduces to

$$D^2 \psi' = 0 \quad (28)$$

Now, the same result would be arrived at if instead of assuming a frictionless fluid, one were interested in the case of zero peripheral component, i.e.,

$$[2\pi \Omega_0 R_0 / Q] = 0 \quad . \quad \text{Thus, the problem of the frictionless incom-$$

pressible fluid is of more than mere academic interest in that it also represents the limiting value for decreasing ratio of peripheral component to through-flow. As stated at the end of Section 5, this becomes important in the study of reactors larger than the HRE.

The solutions of equation (28) for three different positions of the inlet are given in Figures 6, 7, and 8. In each case, the boundary conditions are that ψ' is zero and unity, respectively, on the appropriate region of the surface of the sphere. The numbers on the streamlines are normalized values of the stream function; e.g., 10% of the fluid flows through the space of revolution marked out by streamlines 0.4 and 0.5. In each case, the solution is independent of the magnitude of the peripheral component, provided the peripheral flow is a free vortex.

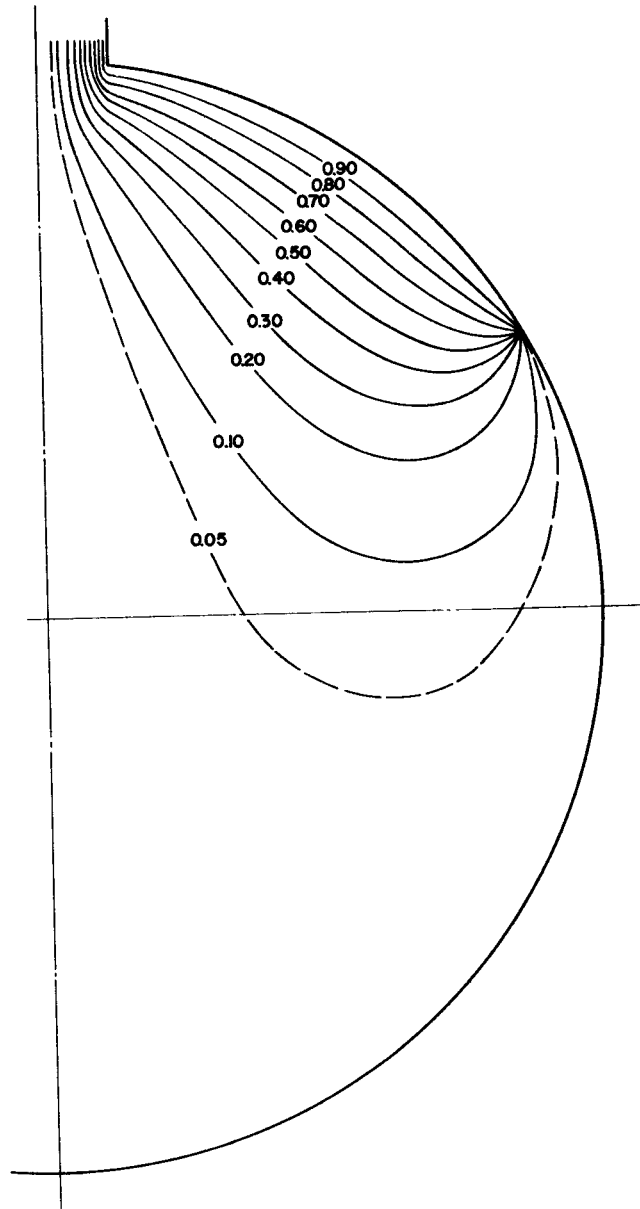


FIG. 6
SOLUTION OF POTENTIAL FLOW
ENTRY AT 30° N. LATITUDE

UNCLASSIFIED

UNCLASSIFIED
DWG. 13851

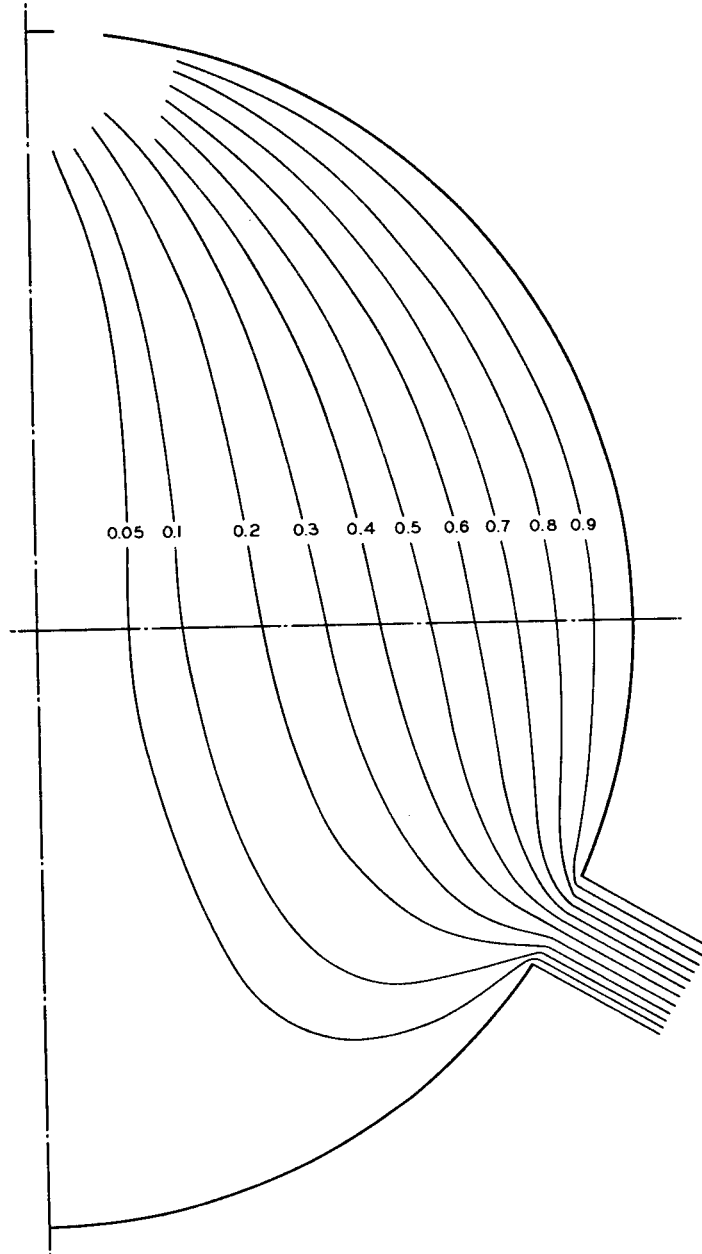


FIG. 7

SOLUTION OF POTENTIAL FLOW
ENTRY AT 30° S. LATITUDE

UNCLASSIFIED

UNCLASSIFIED

UNCLASSIFIED
DWG. 13852

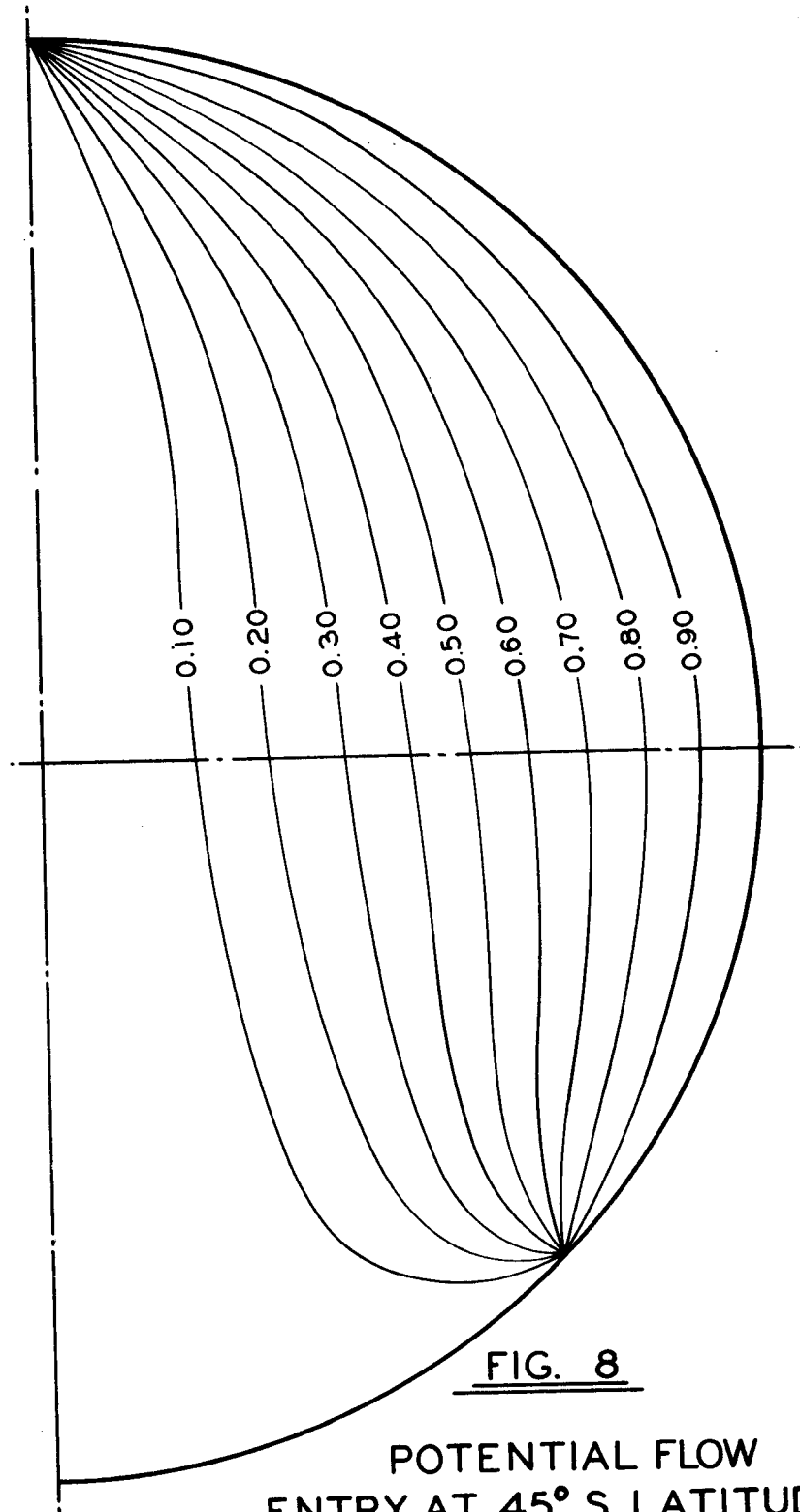


FIG. 8

POTENTIAL FLOW
ENTRY AT 45° S. LATITUDE

UNCLASSIFIED

~~SECRET~~
~~CONFIDENTIAL~~

The solutions were found by a combination of hand and IBM calculating techniques as described in Section 6. The number of interior points used in the finite-difference approximation was 207, corresponding to lattice dimensions of $\Delta\theta = 7.5^\circ$ and $\Delta R' = 0.1$. Fine as this lattice is, it is still too coarse to give detailed information in the immediate vicinities of inlet and outlet. This is not a major difficulty, however, inasmuch as the flow in these regions is relatively insensitive to what is happening in the remainder of the sphere and the solutions for the two singularities (inlet and outlet) can be superposed on the solution for the bulk of the field without any trouble.

The solutions one chooses for these singularities depends on how one idealizes a single inlet pipe into an axi-symmetric inlet. Figures 6 and 8 show the inlet represented by a ring source, while Figure 7 represents the inlet by an annulus whose width equals the actual diameter of the single inlet pipe. In Figure 6, the outlet is represented by a pipe across which the axial velocity is uniform; in Figure 8, it is represented by a point-sink. In any case, the effects of these assumptions are felt only in the immediate vicinities of the singularities.

In Figures 6, 7, and 8, it is assumed that the incoming flow has radial and peripheral velocity components only, but no tangential component. To find the effect of adding a tangential component at the inlet, one may add directly to the previous solution (due to the linearity of the differential equation) the solution to the problem of $\psi' = 0$ everywhere on the surface of the sphere, with an appropriate value of tangential velocity at the location of the inlet. Such a solution is given in closed form by Hill's Spherical Vortex (Refs. 4 and 5). In our notation, it is

~~SECRET~~

$$\psi = A (1 - R'^2) R'^2 \sin^2 \theta \quad (29)$$

where A is a scale factor which determines the strength of the spherical vortex. From equation (29) the maximum value of ψ is $A/4$ and it occurs at $\theta = \pi/2$ and $R' = \sqrt{2}/2$. Figure 9 is a plot of equation (29), in which the maximum value of ψ has been set at unity.

From equation (29),

$$D^2 \psi = -10 A R'^2 \sin^2 \theta$$

Comparing this with equation (23), it is seen that for this spherical vortex, the value of ξ/r is constant over the field (equal to $10A$). Thus, while this spherical vortex is not a potential flow (that is, it has vorticity), it does satisfy the condition for frictionless incompressible flow, that the vorticity be proportional to the distance from the axis of symmetry.

The value of the scale factor A in equation (29) is found from the tangential component of velocity one wishes to match at the inlet. Substituting equation (29) into (7),

$$\begin{aligned} V &= -\frac{1}{R \sin \theta} \frac{\partial \psi}{\partial R} \\ &= -\frac{1}{R_0^2 R' \sin \theta} \frac{\partial \psi}{\partial R'} \\ &= -\frac{2A \sin \theta}{R_0^2} (1 - 2R'^2) \end{aligned}$$

or

$$V_0 = 2A \sin \theta_0 / R_0^2 \quad (30)$$

where V_0 is V at the inlet (i.e., $R' = 1$ and $\theta = \theta_0$). Substituting from equation (30) into equation (29) and normalizing with respect to the

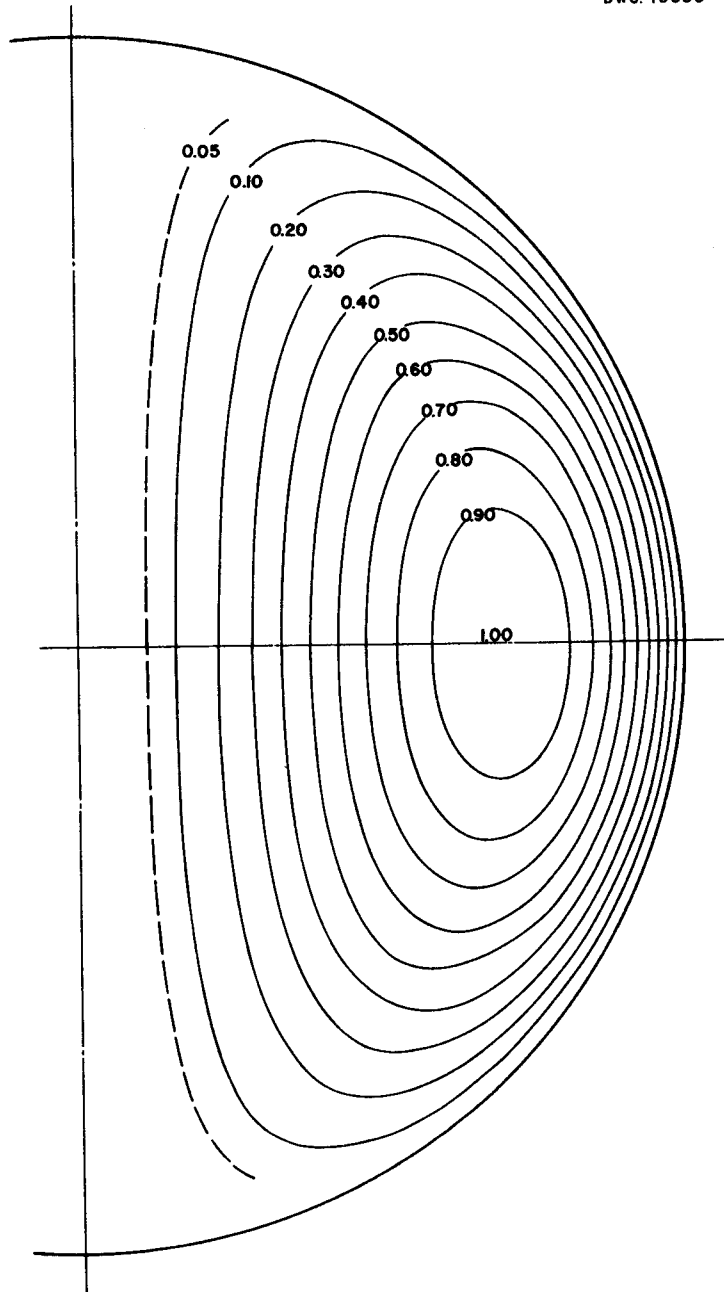


FIG. 9

SPHERICAL VORTEX
IDEAL FLUID

[REDACTED]
SECRET [REDACTED]

total through flow as in Section 4, the stream function due to the spherical vortex is

$$\psi' = \left[\frac{\pi R_o^2 v_o}{Q \sin \theta_o} \right] (1 - R'^2) R'^2 \sin^2 \theta \quad (31)$$

If one now idealizes the inlet pipe by an annulus of width d_o (equal to the diameter of the actual inlet pipe) whose axis makes an angle δ_o with the radial direction, the bracketed term in equation (31) reduces to $\frac{R_o}{2 d_o} \frac{\sin \delta_o}{\sin^2 \theta_o}$, and from this the value of ψ' is easily calculated.

Figure 10 shows the result of such a superposition (for $\delta_o = 30^\circ$) when added to the results of Figure 6. The redistribution of residence times is quite evident; a quantitative estimate of its effect is made below. Figure 11 shows the result of adding the spherical vortex (again $\delta_o = 30^\circ$) to Figure 7. Here the effect of the vortex is so strong that a closed region results. In Figure 12, a value of δ_o is found which gives incipient stagnation with the same location of the inlet.

These effects can be summarized by finding the variation in outlet temperature in each of the problems. Applying equation (21), one finds the following:

Temperature Rise Along a Given Streamline/Average Temp. Rise

	$\psi' = 0.10$	$\psi' = 0.90$
Figure 6	1.98	0.11
Figure 10	1.34	0.23
Figure 7	; 1.49	0.66
Figure 12	1.11	1.03

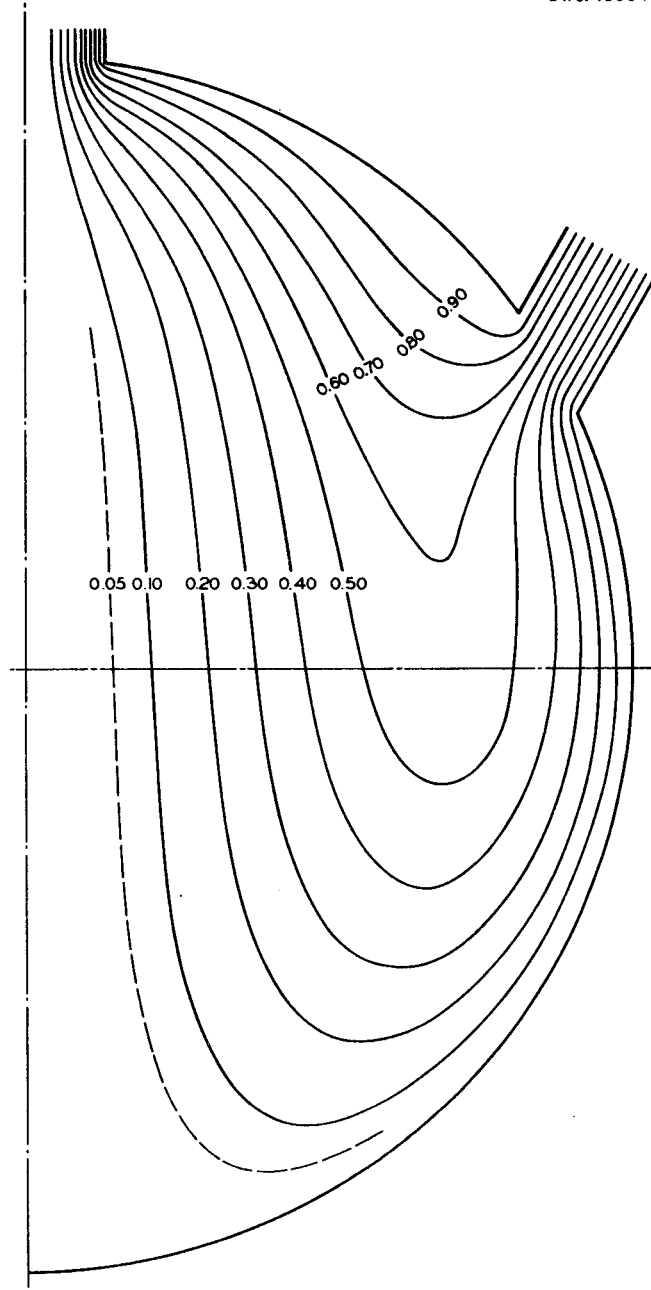


FIG. 10

FRICTIONLESS INCOMPRESSIBLE FLOW
ENTRY AT 30° N. LATITUDE
INLET PIPE AT 30° TO THE RADIAL DIRECTION

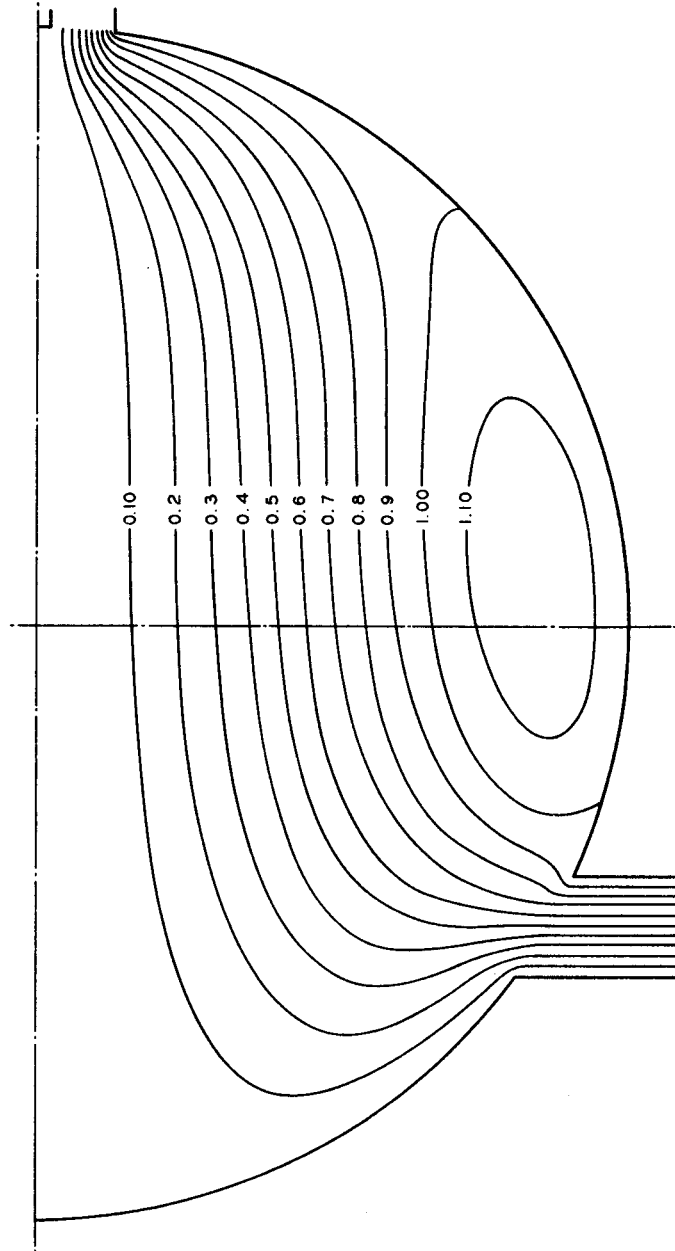


FIG. II

FRICTIONLESS INCOMPRESSIBLE FLOW
ENTRY AT 30° S. LATITUDE
INLET PIPE AT 30° TO THE RADIAL

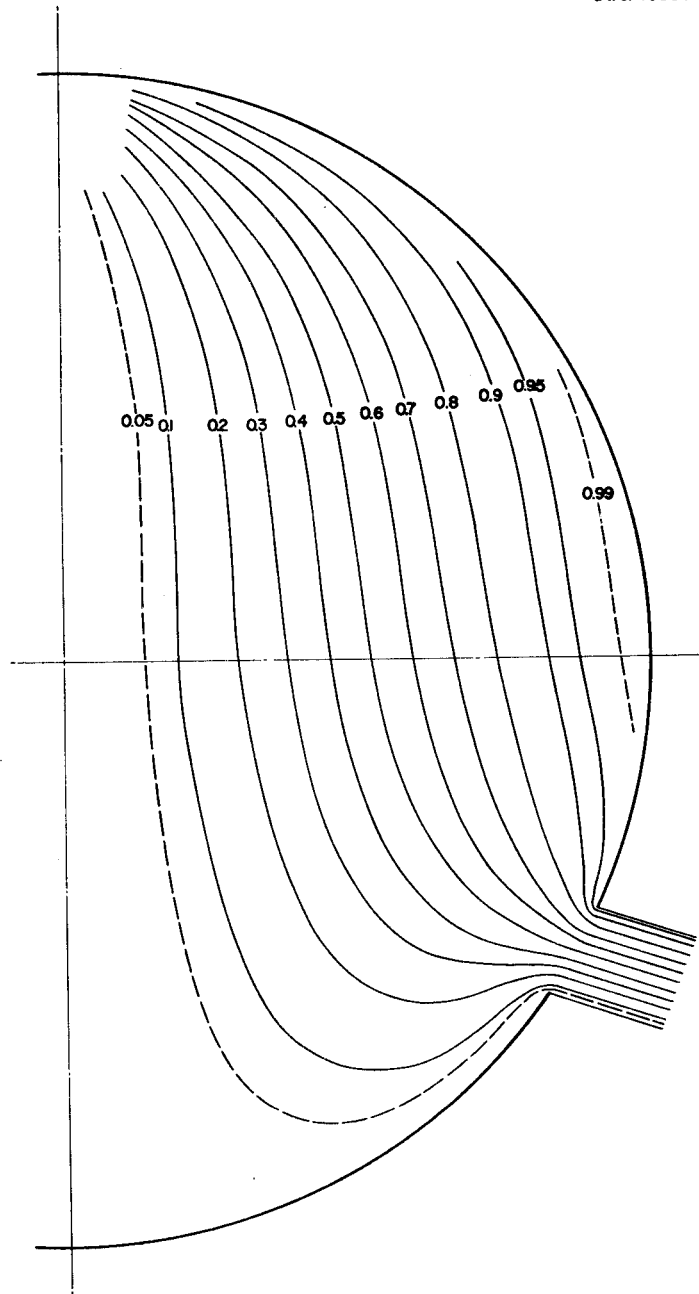


FIG. 12

FRICTIONLESS INCOMPRESSIBLE FLOW
ENTRY AT 30° S. LATITUDE
INLET PIPE AT 11.5° TO THE RADIAL



Bibliography

1. Goldstein, S., ed., "Modern Developments in Fluid Mechanics," pp. 114 - 115, Oxford University Press, Oxford, 1938
2. "ERE Feasibility Report," ORNL-730, p. 63, June 20, 1950
3. Southwell, R. V., "Relaxation Methods in Theoretical Physics," Chapter II, Oxford University Press, Oxford, 1946
4. Milne-Thomson, L. M., "Theoretical Hydrodynamics," 2d ed., p. 495, Macmillan, New York, 1950
5. Lamb, H., "Hydrodynamics," 6th ed., p. 245, Dover, New York, 1945

